Inkjet printing and photonic sintering of silver and copper oxide nanoparticles for ultra-low-cost conductive patterns†

Andreas Albrecht,* Almudena Rivadeneyra, Alaa Abdellah, Paolo Lugli and Jose´ F. Salmero´n

Printing technologies to produce conductive films and electronic devices are well established and employ only inexpensive materials and devices as well as rapid post-processing methods. In this work, silver nanoparticle and copper-oxide nanoparticle ink was printed using a consumer inkjet printer on a large variety of commercially available substrates. The print quality was assessed by various methods. Self-sintering of the silver ink led to sheet resistances of less than 400 mΩ $\square^{-1}$. Photonic sintering reduced the sheet resistance down to 55 mΩ $\square^{-1}$ within a few milliseconds, equivalent to 2.4 times that of bulk silver. Copper oxide ink was reduced by intense pulsed light and a sheet resistance of 335 mΩ $\square^{-1}$, or 4.5 times that of bulk copper, was obtained. The parameters for sintering were optimized for both inks to achieve low resistivities within a few seconds without damaging the substrates. The production process can be reduced to a few minutes and is fully roll-to-roll compatible, thus providing a quick and ultra-low-cost manufacturing method to produce conductive patterns for wiring, printed circuit boards, antennas, sensor electrodes, light emitting diodes, and solar cells.

Introduction

An essential part of every electronic application is its wiring mechanism – its way to electrically connect different components to achieve the desired functionality. Sensors, transistors, and solar cells require electrodes to transport electrons to and from the active areas. Touch screens and antennas are based on conductive patterns to allow the communication with humans and other devices, respectively. All components of a system must be connected with wires typically embedded into a printed circuit board (PCB).[1–3]

Traditional methods to produce conductive patterns involve lithography, a multi-step subtractive process that is incompatible with roll-to-roll production, requires clean room facilities, and produces chemical waste.[4] In contrast, additive printing methods promise high throughput, low-cost, and improved environmental friendliness. Several technologies are applicable to print conductive materials and profit from the wide use and experience in the graphics industry. It is expected that printed electronics can reduce complexity and costs, especially for large areas and line widths greater than 50 μm.[5–7] For rapid prototyping, digital printing technologies, *e.g.* inkjet, are a promising step. Inkjet printing is a contactless process under ambient conditions and almost free of chemical waste. Process speeds are ranging from 1 to 100 m min^{-1}, mainly depending on the inkjet head and the width of substrates.[3,8] Furthermore, the possibility of using well known substrates like paper or polymer films enables flexible, cheap, and disposable devices.

Metallic inks containing gold, silver, copper, aluminium, or others offer a much higher conductivity than polymer-based inks.[2,5,7] Noble metals, *e.g.* silver, are typically dispersed in solvents as nanoparticles (NP) to reduce their melting point.[9] Non-noble metals, *e.g.* copper, tend to rapidly oxidize and are typically printed in a precursor form.[10,11] After printing with any kind of ink, the ink carrier and the functional components must be separated, which can be achieved by evaporation of the ink carrier or its absorption into deeper layers of the substrate.[12,13]

Typically, at least one more post-processing is required to form a conductive layer. Precursor materials, *e.g.* copper oxide (CuO) NP, must be converted into a metal and the electrical connection between the NPs must be established. The latter is achieved by sintering at high temperatures to create conductive necks between the particles and increase their packing density. At least 120 °C or much higher temperatures are necessary[9] that are incompatible with many low-cost substrates. To prevent damage to heat-sensitive substrates, several alternative sintering methods have been developed to selectively heat the printed

Institute for Nanoelectronics, Technische Universität München, Theresienstr. 90, Mu¨nchen, Germany. E-mail: andreas.albrecht@tum.de

† Electronic supplementary information available

pattern and expose the substrate only to moderate temperatures. Electrical sintering uses local Joule heating by resistive energy dissipation, but results in inhomogeneous sintering. Recent developments of contactless sintering heads overcame the challenges in sintering complex structures, however, it requires an initial conductivity.[14–16] Microwave sintering utilizes the energy dissipation at the interaction of conductive patterns with alternating electric fields. It is fast, able to process larger areas, and can achieve a low resistivity but a very homogenous field and an initial conductivity of the pattern is required.[16–20] Laser sintering locally heats the ink within the laser beam. This allows higher process temperatures but is time consuming.[21–23] Intense pulsed light (IPL) sintering is based on the distinctly higher absorption of visible light of metal NPs compared to paper and polymeric films. Intense light pulses of a duration around one millisecond generate local temperatures of up to 1000 °C in thin metal layers to rapidly sinter the NPs. The fast heating leads to a higher densification.[9] The short pulse duration and the low heat conductivity of most substrates reduce the heat transfer and prevent excessive heating of the substrate. Typically, the sintering process requires only a few pulses, can be done at room conditions and is roll-to-roll compatible, which lowers complexity and costs and increases throughput.[5,16,24–27] IPL sintering is, furthermore, able to trigger chemical reactions in the printed layer, *e.g.* the reduction of copper oxide in a specific environment.[28] Novacentrix ICI-002HV ink uses a specific ink formulation that allows the conversion of the copper-oxide nanoparticles to sintered copper in a single step.[12,29,30]

Applications for printed conductors include RFID antennas, circuit boards, and electrodes for organic light emitting diodes, solar cells, and various sensors.[1–3,5,6,31]

This work analyses the influence of substrates and sintering parameters on the electrical properties of conductive inks deposited by inkjet printing. We use a silver and a copper-oxide ink to produce conductive patterns on a wide range of substrates, including paper- and polymer-based materials. Low-cost substrates widely used by consumers and industry are compared to special papers for printed electronics. Ideal sintering parameters are identified to reach high conductivities.

Materials & methods

Inks and printing equipment

The silver (Ag) nanoparticle ink and copper oxide nanoparticle ink were used without processing except for shaking by hand prior to filling the cartridge. The Ag ink DGP-40LT-15C of ANP (Korea) contains 35% silver nanoparticles in TGME (triethylene glycol monoethyl ether) and has a density of 1.45 ± 0.05 g cm^{-3}. The CuO ink ICI002HV of Novacentrix (Texas, US) contains 16% fully oxidized copper nanoparticles.

A low cost consumer inkjet printer, Workforce 2010W of Epson (Japan), was used without further modification for the printing of the samples. The black cartridge was replaced by a refillable cartridge that was filled with silver or copper-oxide nanoparticle inks. The printed pattern contains lines of different widths (50, 100, 200, 300, and 500 μm) in and perpendicular to the moving direction of the printhead, dots of the same diameter, a line with pads as well as a printed area of 5 × 10 mm for sheet resistance measurements (Fig. 1).

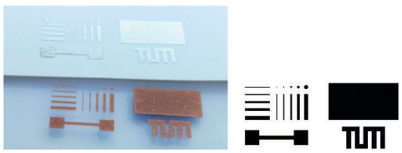

Fig. 1 Left: Inkjet-printed and sintered silver NPs (top) and copper oxide NPs (bottom) on porous substrates. Right: Test pattern containing horizontal and vertical lines and an area for sheet resistance measurements.

Substrates

40 porous paper- and polymer-based substrates were tested in a preliminary study for inkjet printing of both silver and copper inks. The paper-based substrates are a variety of glossy, semi-matte and matte coated photo papers, fine letter paper, low-cost copy paper and two special papers for inkjet-printed electronics. The polymer-based substrates contain inkjet reproduction films, polypropylene-based graphic media, and two special films for inkjet-printed electronics. A selection of 21 substrates was found to be suitable for both inks (see Table S1 in the ESI†). Nine of these substrates are white paper-based (P1 to P9), ten are transparent polymer-based (T1 to T10) and two are white polymer-based (W1 and W2) substrates. All substrates have an ink-absorptive coating.

Furthermore, 22 non-porous substrates were tested for crack-free areas and matching of the substrate's and ink's surface energies. The substrates included special films for printed electronics, photo papers for laser printers, laser and inkjet copy foils, and films for screen printing. Eight of them are presented here: two are white special papers for printed electronics (N1 and N2), three are laser copy papers (N3 to N5), two are laser copy foils (M1 and M2), and one is a screen printing film (M3).

Production process

Before printing the samples, the nozzles were cleaned and it was ensured that no nozzles are blocked or misfiring because of air within the channels. The samples were printed using the printer driver and the following settings: Epson Matte was selected for the paper type and strong for the quality. A finer raster and slow printing were used. The substrate was fed through the built-in paper feed.

For comparison reasons all samples with silver nanoparticles were dried at 65 °C for one hour in an oven. The copper samples were stored for about 30 minutes to dry.

After drying, IPL sintering using a Sinteron 2010 (Xenon, US) was conducted. If not noted otherwise, a double pulse at 2.5 kV and a period of 3 s were used for the printed Ag. The pulse lengths were 1 ms for the first, and 2 ms for the second pulse. The CuO samples were sintered with a single 2 ms pulse at 3.0 kV.

According to the user manual of the Sinteron, the energy to the lamp can be calculated using eqn (1). HV is the set high voltage, and WIDTH is the pulse width.

$$E = \left(\frac{\mathrm{HV}}{3060\,\mathrm{V}}\right)^{2.3} \cdot 938\,\mathrm{J\,ms^{-1}} \cdot \mathrm{WIDTH} \qquad (1)$$

Only a portion of this light reaches the substrate. For an 830 J pulse, the energy density is 3.15–3.38 J $\mathrm{cm^{-2}}$.

Characterization

Optical microscopy images were obtained using a DM 2500 equipped with a DFC295 camera, both of Leica Microsystems (Germany). Profilometer studies have been carried out using a Dektak XT of Bruker (US). Atomic force microscopy (AFM) images were obtained using a JSPM 5200 of Jeol (Japan). Scanning electron microscopy (SEM) images have been obtained using an Nvision 40 of Zeiss (Germany) at 5.0 kV beam energy and a magnification of 25 000. Sheet resistance measurements were conducted on a printed 5 × 10 $\mathrm{mm^2}$ area with a self-made linear four-point probe in combination with a Keithley ACS 4200. A correction factor of 0.651 was calculated and applied to compensate the effect of limited boundaries according to Smits *et al.*[32] Static water contact angles of 4 μL droplets of deionized water were measured under ambient conditions by the sessile-drop method using an OCA15 of Dataphysics (Germany).

Results & discussion

We found that the print quality of both inks is mainly depending on the choice of the substrate. Thus, we show a detailed analysis of the printed silver samples and only highlight the differences of copper inks later in this work. Fig. 1 shows one well-conductive sample for each ink after sintering.

Print quality assessment of Ag patterns

On some substrates, the silver ink immediately creates a shiny silver layer after printing. On others heat-drying is necessary to achieve this layer. On the third group of substrates, the ink remains dark green or shows a very inhomogeneous pattern. Fig. 2 shows optical microscopy images of printed areas of about 1 $\mu\mathrm{m^2}$ Ag NP ink on different substrates. Most porous inkjet media like glossy or semi-matte inkjet photo paper or inkjet reproduction films show a print pattern like on substrate T8 in Fig. 2a. Individual drops are perceptible and cover the entire area. Fig. 2b shows the print pattern on a very smooth non-porous polymer film. No individual drops are visible as the ink remains liquid after printing and solidifies during drying. Fig. 2c shows a rougher non-porous polymer film that is disturbed by stains of different sizes. All these three surfaces exhibit a shiny silver which is shown with a higher brightness than the substrate in the microscopy images.

Some substrates, for example, letter or copy paper, matte photographic paper, and polypropylene-based graphic films show a dry but dark surface which presumably originates from an absorption of both the ink carrier and the metallic NPs.

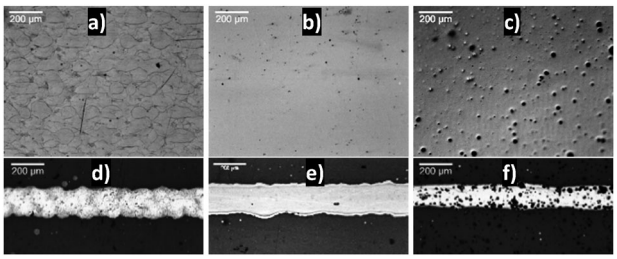

Fig. 2 Microscopy images of printed areas (a–c) and lines (d–f) on different substrates: porous inkjet media P9 (a & d), smooth non-porous film M1 (b & e), and laser printer foil M1 (c & f). All these three surfaces exhibit a shiny silver layer that results in a higher brightness of the ink-covered areas in the microscopy images. Scale bar: 200 μm.

Optical microscopy images of a printed silver film on unsuitable substrates are shown in the ESI.† Negative effects are too large pores that absorb ink and solvent or a mismatch of surface tensions of the ink and the wettability of the substrate that leads to cracks or ink agglomerates.[33]

Another important criterion for printed electronics is the quality of printed lines. Fig. 2d–f show optical microscopy images of lines with a designed width of 100 μm of Ag NP ink on a selection of substrates. Fig. 2d shows a line composed of ink droplets on porous inkjet media (P9). A drop gain of 50 μm was observed for all line widths, which is assumed to be related to missing dot gain compensation mechanisms in the ultra-low-cost printer. Some non-porous media show a uniform line as depicted in Fig. 2e. However, the surface energy matching of ink and the film as well as the quality of the film must be high to obtain a line with homogeneous edges. Rough films may contain stains (Fig. 2f) that increase the resistance of the line. If the wettability does not match the surface energy of the ink, dot gains may increase or the ink agglomerates to separate drops.

A rough estimation of the amount of silver present on a specific area was done by cutting two non-porous films to the identical area. Both were weighed directly after printing of Ag NP ink on one of them without drying. The average additional weight of the printed silver was 1.19 ± 0.24 mg per square centimetre of the printed pattern. This means that a volume of 8.19 ± 1.64 nL was applied to an area of one square millimetre. With the density of bulk silver of 10.49 g $\mathrm{mL^{-1}}$ and the silver content of the ink, 30–35 wt%, the minimal film thickness that could be achieved is in the order of 368 ± 79 nm.

Due to pores resulting from non-perfect packing, the real thickness is expected to be much higher. We measured it on one of the smoothest substrates T8 and revealed an average film thickness of 696 nm at a roughness of 111 nm. The measured thickness can be explained by a porosity that leads to an average density of 50.5% ± 10.9% of the density of bulk silver, *i.e.* 5.29 ± 1.14 g $\mathrm{mL^{-1}}$ that is comparable to other literature studies.[9,34]

Fig. 3a shows a SEM image of the printed silver NP layer on substrate P7 without sintering. Silver NPs of about 50 nm in diameter form a rough but homogenous layer. No large cracks are visible within the sample and only a few droplet borders are

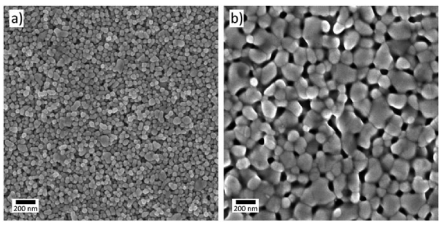

Fig. 3 SEM images of silver NP ink (a) after drying without sintering and (b) after sintering on substrate P7.

perceptible at large area scans. This indicates a high print quality and no formation of "coffee stain" rings.[35] The diameter of the NPs increases approximately by a factor of four after photonic sintering with two 2 ms pulses at 2.5 kV as shown in Fig. 3b. Similarly, the sintered sample shows no cracks and the droplet borders vanished completely.

Ag NP ink on porous substrates

Porous substrates are well suitable for inkjet-printing because they absorb the ink carrier but not the nanoparticles, if the pore sizes are small enough.[12,36] AFM images of some substrates to estimate the pore size and their roughness are provided in the ESI.† Inkjet printing of nanoparticles on porous substrates results in an instantly dry silver NP layer above the substrate with straight line contours. On some substrates this layer is immediately conductive. After drying for one hour, all selected substrates are conductive. The conductivity varies across almost one order of magnitude. The lowest sheet resistance without any methods of sintering lies at around 385 mΩ $\square^{-1}$ (sample P8 and P17). The dark blue bars in Fig. 4 show that most measured values do not exceed 5 Ω $\square^{-1}$. Assuming a thickness of 696 nm, a conductivity of 6% of bulk silver could be reached without sintering. We found that the resistance corresponds in most cases to the visual impression. Only shiny silver layers showed a high conductivity whereas darker layers exhibit a high resistivity. It was found that the creation of shiny layers mainly depends on the surface of the substrate and the separation of the ink components. Generally speaking, the ink carrier needs to be separated from the nanoparticles to obtain the prerequisites for conductivity.

However, photonic sintering is able to reduce the resistance by 75% to 99% to values between 55.4 mΩ $\square^{-1}$ (sample P7) and 195 mΩ $\square^{-1}$ (T4). Sample P3 has the second lowest resistance of 61.1 mΩ $\square^{-1}$ but has a smoother surface than P7. Assuming a thickness of 695 nm, the sample with the highest conductivity reached 42% (P7) of bulk silver. The standard deviation between the different substrates is reduced from about 85% to 40% of the mean value. Fig. 4 shows the sheet resistances of inkjet-printed silver nanoparticles on all 20 suitable substrates before (Ag printed) and after (Ag sintered) sintering.

The parameters of the IPL sintering are crucial for the resulting resistance and the destruction of the printed pattern. For a more detailed evaluation, samples were printed on substrate P7 and sintered under different conditions. In order to cover the operation range of the Sinteron, the voltage was fixed at five levels between 2.00 kV and 3.00 kV in steps of 0.25 kV and the pulse duration was varied between 250 μs and 3000 μs.

First, we present the resistance measurements for each sample (Fig. 5a). Experimental values are shown by markers. The lowest sheet resistances of 82 mΩ $\square^{-1}$ and 88 mΩ $\square^{-1}$ are obtained for 2000 μs pulses at 2.75 kV and 2.50 kV, respectively. The lowest value for each power is below 140 mΩ $\square^{-1}$, indicating that lower power can be compensated by longer pulse duration. The decrease of resistance follows an exponentially decaying relation with offset (parameters a, b, and c) of the form of eqn (2) and is shown in the figure as continuous lines.

$$R_S = a \cdot \exp(-b \cdot x) + c \quad (2)$$

here, x describes the pulse duration. Above a certain exposure level, the entire pattern gets completely destroyed and the measured sheet resistance is higher than 1 MΩ $\square^{-1}$. The steeply inclining lines in the figure indicate the complete destruction of the sample at the next higher pulse width. Furthermore, Fig. 5a shows that the resistance can be modelled as a linear relationship with the power of the lamp for all pulse widths up to a certain exposure level at which the pattern was blown off. For low pulse widths, the resistance heavily depends on the power of the pulse.

Fig. 5b shows the sheet resistance values plotted across the energy to the lamp. We found that most experimental values are lying on a similar exponentially decaying curve of the form of eqn (2) with x describing the energy of the pulse and the parameters a = 3268 ± 346 mΩ $\square^{-1}$, b = 8661 ± 809 J^{-1},

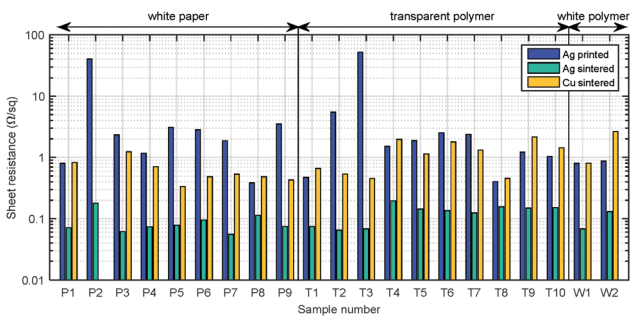

Fig. 4 Sheet resistance of inkjet-printed silver nanoparticles before and after sintering and copper-oxide nanoparticles after sintering on porous substrates.

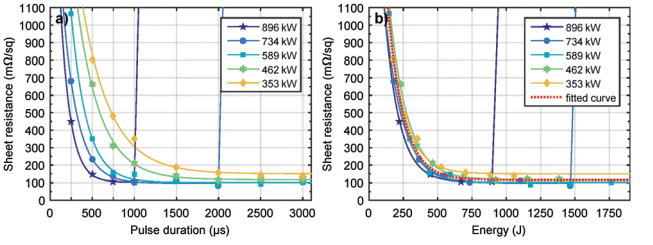

Fig. 5 Sheet resistances of printed Ag NP ink on substrate P7 after sintering with different pulse durations and powers. Markers show experimental values with fitted exponentially decaying lines in the same colour. (a) Exponentially decreasing relationship between pulse duration and resistance and linear decrease between power and resistance. (b) Exponential decrease of sheet resistance to higher energy almost independent of power.

and c = 115.5 ± 22.6 mΩ $\square^{-1}$ (including 95% confidence interval). This curve is plotted as a red dotted line. It was observed that the obtained resistance mainly depends on the energy to the lamp rather than the power. Following this equation, the resistance for sintering energies above 1000 J is less than one percent higher than the lowest value.

The second important criterion is the destruction of the sample caused by the high-energetic pulses. The destruction grade of the samples was evaluated using the following scheme. Grade 1 indicates visually perfectly intact structures in all parts of the test pattern. Grade 2 indicates minor damage of a diameter larger than the thinnest line (approx. 50 μm). Grades 3 to 6 indicate damage of a diameter larger than the 100, 200, 300, 500 μm line in this order. Grade 7 indicates major damage that makes it difficult to measure the sheet resistance, and Grade 8 corresponds to the complete destruction of the conductive film.

Fig. 6a shows the relationship between the destruction grade and the pulse duration for the power values. At all powers, the samples sintered with a 250 μs pulse do not show any damage. The longer the pulse duration is, the more distinctive the destruction is. Already a 500 μs pulse shows damage at the highest power value used. For pulse widths of more than 1500 μs, a clear difference is observed between low and high power values. Whereas low power pulses (<500 kW) leave the pattern intact, high power pulses (>500 kW) destroy the pattern severely. We observed, that the destruction for high power values follows the energy to the lamp, but for low values, the pattern remains intact also at much higher energy.

The obtained resistance and the destruction grade are the most important characteristics of the sintering of a printed conductive pattern. The most favourable combination for most applications of the films as conductors has both values very low. This work proposes a simple figure of merit, the quality rating Q: the sheet resistance R_S is normalized to the minimal achievable sheet resistance and multiplied by the destruction level D. The lower the quality rating, the better compromise could be found between these two criteria. This method assumes that the destruction of the thinnest line (Grade 1) is equally important for the application to a double resistance. In general, the destruction grade D can be compensated by a reduction of the sheet resistance R_S to $1/D$. The model can be modified by exponentiation of one of the two components to better fit specific applications.

$$Q = \left(\frac{R_S}{\min(R_S)}\right)^a \cdot D^b \tag{3}$$

here we want to use the model with $a = b = 1$. Fig. 6b shows the quality rating as functions of pulse duration. The figure shows that the best compromise between resistance and the destruction grade according to this model lies at 500 μs for 3.00 kV and 2.75 kV pulses, 750 μs for 2.5 kV pulses, and 2000 μs for 2.25 kV and 2.00 kV pulses. The ideal value shifts to higher pulse durations for lower voltages and power values. High-power pulses (>500 J) have their best quality rating at around 350 J, whereas low power pulses have it around 1000 J.

Following this model, the ideal photonic sintering parameters for a single pulse are a duration of 2000 μs at 2.25 kV, relating to pulse of 935 J at 462 kW. A pulse of 750 μs at 2.5 kV leads to comparable results with half the energy consumption (442 J at 589 kW). Assuming that the energy delivered to the sample scales proportionally to the energy to the lamp, an energy density of approximately 1.75 J cm^{-2} is applied in the latter pulse.

The resistance can be further reduced by a second pulse. This was investigated for two different powers, 734 kW and 589 kW. For the first pulse, the longest pulse duration that did not destroy the sample was used. This is 500 μs and 750 μs, respectively. The second pulse duration was then increased up to 3000 μs. The sheet resistances reduce with higher pulse duration to values as low as 90 mΩ $\square^{-1}$ as shown in Fig. 7a.

There is a reduction of 61% or 43% compared to the resistance value measured after the first pulse. Furthermore, the destruction of the sample occurred at much higher energies as can be seen in Fig. 7b. The samples sintered at 589 kW withstand pulse durations of 3000 μs without any damage and achieve a low resistance. The quality rating improves significantly for the two powers tested. Very low 90 mΩ $\square^{-1}$ can be reached without damage at 589 kW with a first pulse of 750 μs and a second pulse of 3000 μs. Further sintering pulses did not show a decrease of the resistance, so it is assumed that 90 mΩΩ $\square^{-1}$ is already very close to the practical optimum. Assuming an effective thickness of 368 nm as calculated above, this is 42% of the bulk conductivity.

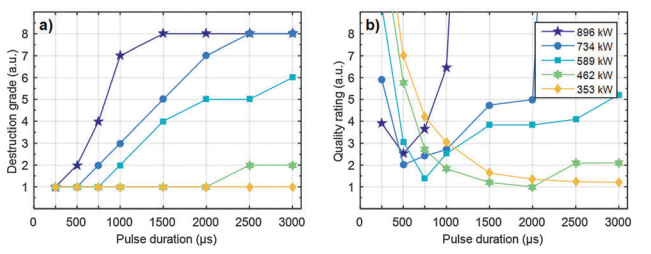

Fig. 6 Dependency of (a) destruction grade and (b) quality rating of printed Ag NP ink on substrate P7 after sintering to the duration of the pulse. Markers show experimental values with connecting linearly interpolated lines in the same colour. The legend applies to both graphs.

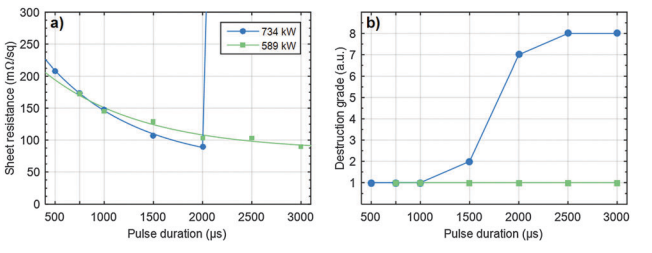

Fig. 7 (a) Sheet resistances and (b) destruction grade of printed Ag NP ink on substrate P7 after sintering with a first pulse of 500 μs at 734 kW and 750 μs at 589 kW, respectively, and then sintered with a second pulse at different pulse durations with the same power. The legend applies to both graphs.

Ag NP ink on non-porous substrates

Non-porous substrates do not absorb the ink carrier and, thus, require further post-processing of the samples before sintering. We heated the substrate in an oven for one hour to 65 °C, which is sufficient to evaporate the solvent but not deform the substrate. On some substrates, the printed pattern starts spreading, which lowers the field of application for this substrate. On some samples, *e.g.* N2 with a high contact angle of about 95° for water, the ink agglomerates to larger but separate drops. On the best substrates, a homogeneous and shiny silver layer appears after drying with sharp and straight edges according to the designed pattern. This can be achieved on some papers and films intended for laser copiers. Before sintering, the sheet resistance varies across many orders of magnitude as shown in Fig. 8a. The paper-based samples show sheet resistances above 1 kΩ $\square^{-1}$ (N3 to N5) and sample N2 is not conductive at all.

In contrast, samples M1 and M2 show a sheet resistance of about 2 Ω $\square^{-1}$ comparable to the non-sintered porous samples. IPL sintering can reduce the resistance across multiple orders of magnitude (Fig. 8b). The sheet resistance of the samples P4 to P6 could be reduced from several kΩ $\square^{-1}$ by 4 orders of magnitude during photonic sintering. The lowest sheet resistance of 150 mΩ $\square^{-1}$ is measured on sample N7 (−93%). This value is considerably higher than the one found on porous substrates, which may result from a more inhomogeneous coverage, and is consistent with the study of Schuppert *et al.*[37] Sample N2 is not conductive due to the separation of the ink into drops.

Print quality assessment of CuO patterns

The colour of the printed CuO is dark brown on all printed substrates. On porous substrates, the ink is instantly dry and slightly maroon. On non-porous substrates, the ink remains wet and dark-brown after drying. We found that the print quality of printed CuO samples is very closely related to Ag samples. On porous media, we can achieve uniform and only slightly wider lines than designed. On non-porous media, the wettability of the substrate influences the uniformity of lines and can disrupt printed areas.

Fig. 9a shows a SEM image of the completely dried CuO ink on substrate T8. The flaky structure probably consists of copper oxide flakes of 120 nm as indicated in the datasheet of the ink and the dried reduction agent or its degradation products. Artefacts in the image are related to the high resistivity of

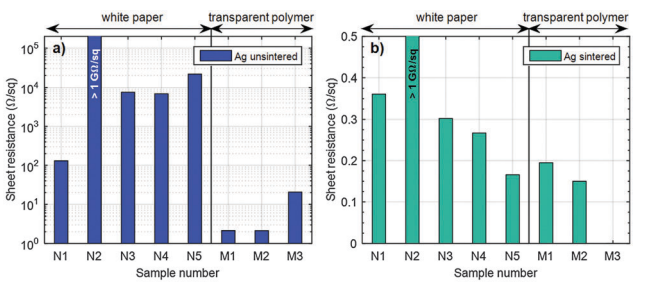

Fig. 8 Sheet resistance of inkjet-printed silver nanoparticles before (a) and after (b) sintering on non-porous substrates.

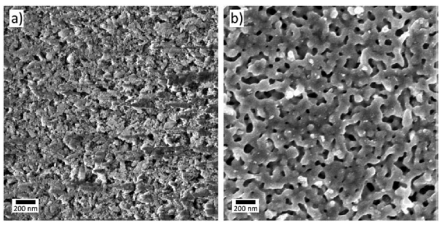

Fig. 9 SEM images of CuO ink (a) after drying and (b) reduced Cu after sintering on substrate P17.

CuO and the coated PET-based substrate. Photonic sintering massively changes the structure as shown in Fig. 9b.

A sponge-like, porous network of copper has been formed, in contrast to the large particle-based network of sintered silver NPs shown in Fig. 3b. Comparable samples sintered at energies higher than the optimum show cracks running through the sintered copper. Furthermore, circular blow-ups can be found that are most probably related to liquids evaporated during the sintering.[36] In comparison to other groups using a different printer, it seems that the drop distribution of the consumer inkjet printer creates a more uniform pattern that reduces the susceptibility to cracks along droplet borders.[38]

A rough calculation of the height of bulk copper expects a value around 130 ± 26 nm. It assumes that the printer applies the same volume of ink for every type of ink, 819 nL cm^{-2} as calculated above and a density of 1.1 g cm^{-3} for the copper-oxide ink. Based on the atomic weights of copper and copper oxide, a copper content of 12.8% (wt) was used for the calculation. The thickness of the film is much thinner than that of the silver film, because of the lower concentration of copper in the ink. The thickness of the film was measured on one of the smoothest substrates T2. It revealed an average film thickness of 212 nm at a high roughness of 37 nm.

The samples printed with CuO ink are more difficult to visually assess than for the silver ink. However, only the porous substrates could be used for producing conductive patterns. Only these substrates facilitate the separation of ink carriers and nanoparticles. Paquet *et al.* found that the optimal separation on Novele PET (also used for sample P11) is achieved about 10 to 30 min after printing and later on the reducing agent degrades and inhibits a successful reduction.[12] In contrast, we did not see any significant relationship between the drying time and the resistance. Nevertheless, we left the samples with the 5 × 10 mm areas for about 30 min in air under room conditions.

CuO ink on porous substrates

Before IPL sintering, all samples are non-conductive. After sintering the suitable substrates show a clear copper-coloured pattern whereas unsuitable substrates do not change their colour, and exhibit a burned-in pattern accompanied by a harsh smoky smell, or the printed pattern blows off. The sheet resistances on most suitable substrates show a variation across one order of magnitude starting at low 335 mΩ $\square^{-1}$ (P5). This relates to a conductivity of about 23% of that of bulk copper.

Most photo papers and some of the coated PET films show sheet resistances at around 500 mΩ $\square^{-1}$. The sheet resistances of printed films on transparent porous films range from 454 mΩ $\square^{-1}$ (T3) to 2155 mΩ $\square^{-1}$ (T9). The values for all films are shown together with the silver samples in Fig. 4.

Similar to silver NP ink, the parameters for IPL sintering of the CuO NP ink are crucial. In order to study this, several samples were printed and sintered at different pulse durations and voltage levels as well as a different number of pulses. Afterwards, the sheet resistance was measured.

All samples sintered at 896 kW and 734 kW are immediately conductive for pulse widths of more than 1500 μs and 2000 μs, respectively. Pulses at medium powers needed a second pulse to obtain a conductivity below 1 Ω $\square^{-1}$. At lower sintering energies the colour of the printed patterns is still a mixture of copper and copper-oxide (dark-green) whereas at higher sintering energies cracking and formation of tombstones occur around the limits of the drops. Pulses of 1000 μs and 1500 μs at 734 kW and 589 kW, respectively, needed up to 10 pulses to reach values below 2 Ω $\square^{-1}$. For pulses for powers of 462 kW and lower, no conductivity was obtained up to ten pulses.

For all samples except one, additional pulses increased the resistance as shown in Fig. 10a and in the ESI.† The higher resistances are caused by cracks and blow-ups. The best sintering parameter to obtain a low resistance is a pulse of 2 ms at 896 kW. This resulted in a sheet resistance of 355 mΩ $\square^{-1}$. This is in contrast to other groups that achieved the best results after several pulses.[12,38] For a further investigation, all samples are compared with the scheme used for the Ag NPs above. Fig. 10 shows that the sintering of the CuO ink follows different trends from the Ag NP ink. The increase of the pulse duration is related to a decrease of the resistance only for low powers as shown in Fig. 10a. However, a clear decrease of resistance at increasing powers for pulse widths of 2000 μs and below can be found (Fig. 10b). Higher pulse widths show a minimum resistance at 734 kW.

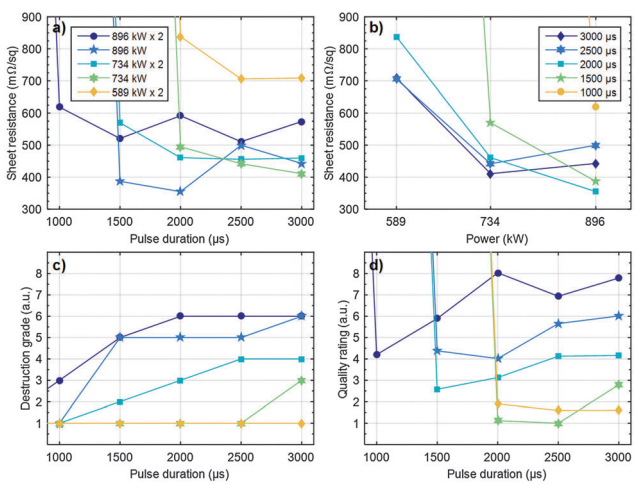

Fig. 10 (a and b) Sheet resistances of printed CuO NP ink on substrate P5 after sintering with different pulse durations (a) and powers (b). (c and d) Destruction grade (c) and quality rating (b) of printed CuO NP ink on substrate P5 after sintering with pulse duration. The legend of the first graph applies to (a), (c) and (d).

The evaluation of the destruction grade is very clear for printed CuO patterns. We applied the same grading system then for the silver printed patterns above. Grade 1 means that the entire pattern is conserved during sintering. Grades 2 to 6 describe damage of the size of 50, 100, 200, 300, and 500 μm, respectively. We found that if the pattern is damaged, the destruction always occurs at the edges of lines and areas. Thus, mainly thinner lines are affected and large patterns are not blown off the porous substrate even at high powers. Fig. 10c shows a clear dependence on the pulse width and power. High pulse durations as well as high powers lead to a destruction of the sample. Powers of 734 kW destroy thin lines of the pattern already at the lowest pulse-width required for obtaining conductivity. Low-power pulses do not harm the pattern at all. The quality rating was calculated as described. The lower destruction grade of the sample sintered with one 2500 μs pulse at 734 kW compared to the one sintered with one 2000 μs pulse at 896 kW clearly predominates the higher sheet resistance of 442 mΩ $\square^{-1}$ compared to 335 mΩ $\square^{-1}$ (Fig. 10d). If the copper-oxide ink is used to print patterns with line-widths of multiple millimetres, the quality rating could be modified. Using $a = 5$ and $b = 1$, the lower destruction grade of the former is compensated by the lower resistance of the latter. Both IPL sintering parameter sets have the same energy consumption. For most applications, sintering with one pulse of 2500 μs at 2.50 kV will give ideal results, although not the lowest sheet resistance.

CuO ink on non-porous substrates

We tried photonic sintering of wet and thermally dried copper oxide printed onto all available non-porous substrates without being able to achieve high conductivity and acceptable copper layers although the CuO ink of Novacentrix is supposed to be suitable for non-porous substrates.[30] Both approaches are showing similar results: if the photonic sintering energy is too low, no conductivity is achieved. If the energy is too high, the pattern is blown off directly. To our knowledge, other groups face the same problems with the ink and could not achieve highly conductive patterns on non-porous substrates. We think that the problem originates from the necessity to separate the ink carrier from the nanoparticles and the reduction agents. Photonic drying seems to be able to dry the samples fast enough to achieve a flat copper oxide layer that can be cured by high-energetic IPL without being blown off. We tried flash frequencies up to the maximum of the Sinteron with varying numbers of pulses followed by one strong pulse to convert the oxide NPs to copper. Optical inspection of the cured samples shows a high degree of damage in all parts of the patterns and presumably a high content of copper oxide in the layers. This leads to a considerably high sheet resistance of about 10 Ω $\square^{-1}$. We think that an optimized drying step by means of IPL drying with high frequency pulses may lead to better results.

Conclusions

Printing of silver nanoparticle ink on photo paper or coated polyester film without any post-treatment gives a sheet resistance

of 400 mΩ $\square^{-1}$. This work showed that drying at only 60 °C achieved a sheet resistance as low as 385 mΩ $\square^{-1}$ on some porous substrates. The sheet resistance of nonporous substrates lies as low as 2.15 Ω $\square^{-1}$ after drying at 60 °C. Much lower resistances can be achieved by intense pulsed light sintering. Sheet resistances of down to 55.4 mΩ $\square^{-1}$ on substrate P7 were achieved with only two pulses of IPL sintering. This relates to a conductivity of 42% of bulk silver in the 696 nm thick film. To achieve the lowest resistance and no damage to the printed pattern, a pulse of 750 μs followed by a pulse of 3000 μs at 734 kW are ideal. This leads to a sheet resistance of 89.8 mΩ $\square^{-1}$ (26% of bulk conductivity) and a printed pattern without any visible damage. Non-porous substrates are more sensitive to ablation of the printed layer and forbid high sintering energies.

The price of printing can be reduced using copper inks, *e.g.* the CuO ink with a light-triggered reduction agent. The best IPL sintering condition to achieve lowest resistances is one high-energetic pulse of 2000 μs at 896 kW, the maximum power achievable with our setup. With this setting, sheet resistances as low as 335 mΩ $\square^{-1}$ were achieved in a 212 nm thick film, which relates to a conductivity of 22% of bulk copper. If a fine pattern must be sintered, it is recommended to reduce the power to 734 kW and use a 2500 μs pulse.

The production of conductive films on flexible substrates does not require expensive materials and time-consuming post-processing anymore. The prices for small quantities of silver ink are less than a euro per printed square decimetre, for the copper ink it is only a few cents for small quantities. Without any post-processing, printed conductors for sensors, electrodes and wiring can be produced. Intense pulsed light sintering equipment costs scale down to less than one euro per printed square decimetre already after printing 1000 m^2. The throughput of inkjet printers and the IPL sintering machines are extremely high compared to most other production methods for patterned conductors. Together with creative ideas for energy supply like bendable batteries and/or harvesting, printed electronics are realisable already today.

Acknowledgements

This work was partly supported by the TUM Graduate School (TUM GS), the Free State of Bavaria under the program ''Solar Technologies go hybrid'' and the DFG Excellence Cluster ''Nanosystems Initiative Munich'' (NIM).

References

1 Y. Kawahara, S. Hodges, N.-W. Gong, S. Olberding and J. Steimle, *IEEE Pervasive Comput.*, 2014, **13**, 30–38.
2 L. Xie, *Heterogeneous Integration of Silicon and Printed Electronics for Intelligent Sensing Devices*, 2014.
3 R. Abbel, P. Teunissen, E. Rubingh and T. Van Lammeren, *Transl. Mater. Res.*, 2014, **1**, 015002.
4 R. Zichner, J. Hammerschmidt, D. Weise, E. Sowade and R. R. Baumann, *TheIJC*, 2014.
5 M. Nir, D. Zamir, I. Haymov and L. Ben-Asher, in *The Chemistry of Inkjet Inks*, ed. S. Magdassi, 2010, pp. 225–254.
6 Y. Kawahara, S. Hodges, B. S. Cook, C. Zhang and G. D. Abowd, *UbiComp'13*, Zurich, Switzerland, 2013, pp. 363–372.
7 Y. Neuvo and S. Ylönen, *Bit Bang: rays to the future*, Helsinki University of Technology, 2009.
8 D. Tobjörk and R. Österbacka, *Adv. Mater.*, 2011, **23**, 1935–1961.
9 G. Bai, PhD thesis, Virginia Polytechnic Institute and State University, 2005.
10 J. S. Kang, H.-S. Kim, J. Ryu, H. Thomas Hahn, S. Jang and J. W. Joung, *J. Mater. Sci.: Mater. Electron.*, 2010, **21**, 1213–1220.
11 K. Woo, Y. Kim, B. Lee, J. Kim and J. Moon, *ACS Appl. Mater. Interfaces*, 2011, **3**, 2377–2382.
12 C. Paquet, R. James, A. J. Kell, O. Mozenson, J. Ferrigno, S. Lafrenière and P. R. L. Malenfant, *Org. Electron.*, 2014, **15**, 1836–1842.
13 D. Sette, PhD thesis, Université de Grenoble, 2014.
14 J. Niittynen, R. Abbel, M. Mäntysalo, J. Perelaer, U. S. Schubert and D. Lupo, *Thin Solid Films*, 2014, **556**, 452–459.
15 M. L. Allen, M. Aronniemi, T. Mattila, A. Alastalo, K. Ojanperä, M. Suhonen and H. Seppä, *Nanotechnology*, 2008, **19**, 175201.
16 S. Wünscher, R. Abbel, J. Perelaer and U. S. Schubert, *J. Mater. Chem. C*, 2014, **2**, 10232–10261.
17 Y. Galagan, E. W. C. Coenen, R. Abbel, T. J. van Lammeren, S. Sabik, M. Barink, E. R. Meinders, R. Andriessen and P. W. M. Blom, *Org. Electron.*, 2013, **14**, 38–46.
18 J. Perelaer, B.-J. de Gans and U. S. Schubert, *Adv. Mater.*, 2006, **18**, 2101–2104.
19 J. Perelaer, R. Abbel, S. Wünscher, R. Jani, T. Van Lammeren and U. S. Schubert, *Adv. Mater.*, 2012, **24**, 2620–2625.
20 J. Perelaer, M. Klokkenburg, C. E. Hendriks and U. S. Schubert, *Adv. Mater.*, 2009, **21**, 4830–4834.
21 S. H. Ko, H. Pan, C. P. Grigoropoulos, C. K. Luscombe, J. M. J. Frechet and D. Poulikakos, *Nanotechnology*, 2007, **18**, 345202.
22 T. Kumpulainen, J. Pekkanen, J. Valkama, J. Laakso, R. Tuokko and M. Mäntysalo, *Opt. Laser Technol.*, 2011, **43**, 570–576.
23 A. Chiolerio, G. Maccioni, P. Martino, M. Cotto, P. Pandolfi, P. Rivolo, S. Ferrero and L. Scaltrito, *Microelectron. Eng.*, 2011, **88**, 2481–2483.
24 I. M. Hutchings and G. D. Martin, *Inkjet Technology for Digital Fabrication*, 2012.
25 A. Kamyshny, J. Steinke and S. Magdassi, *Open Appl. Phys. J.*, 2011, **4**, 19–36.
26 J. Felba and H. Schaefer, *Nanopackaging*, 2008, pp. 239–263.
27 G. Cummins and M. P. Y. Desmulliez, *Circuit World*, 2012, **38**, 193–213.
28 J. Ryu, H.-S. Kim and H. T. Hahn, *J. Electron. Mater.*, 2010, **40**, 42–50.

29 V. Akhavan, K. Schroder, D. Pope, I. Rawson, A. Edd and S. Farnsworth, *Reacting Thick-Film Copper Conductive Inks with Photonic Curing*, 2013.
30 NovaCentrix, Metalon ICI-002HV, 2012.
31 R. Vyas, V. Lakafosis, A. Rida, N. Chaisilwattana, S. Travis, J. Pan and M. M. Tentzeris, *IEEE Trans. Microwave Theory Tech.*, 2009, **57**, 1370–1382.
32 F. M. Smits, *Bell Syst. Tech. J.*, 1958, **37**, 711–718.
33 *The Chemistry of Inkjet Inks*, ed. S. Magdassi, The Hebrew University of Jerusalem, 2009.
34 J. West, M. Carter, S. Smith and J. Sears, *Intechopen*, 2009.
35 R. Deegan, O. Bakajin, T. Dupont, G. Huber, S. Nagel and T. Witten, *Phys. Rev. E: Stat., Nonlinear, Soft Matter Phys.*, 2000, **62**, 756–765.
36 T. Öhlund, A. K. Schuppert, M. Hummelgård, J. Bäckström, H.-E. Nilsson and H. Olin, *ACS Appl. Mater. Interfaces*, 2015, **7**, 18273–18282.
37 A. Schuppert, M. Thielen, I. Reinhold and W. A. Schmidt, *NIP Digit. Fabr. Conf.*, 2011, **2011**, 437–440.
38 H. Kang, E. Sowade and R. R. Baumann, *ACS Appl. Mater. Interfaces*, 2014, **6**, 1682–1687.